Increased L-[1–^{11}C] Leucine Uptake in the Leptomeningeal Angioma of Sturge-Weber Syndrome: A PET Study

Bálint Alkonyi, MD, Harry T. Chugani, MD, Otto Muzik, PhD, Diane C. Chugani, PhD, Senthil K. Sundaram, MD, William J. Kupsky, MD, Carlos E. Batista, MD, Csaba Juhász, MD, PhD

From the Carman and Ann Adams Department of Pediatrics (BA, HTC, OM, DCC, SKS, CEB, CJ); Department of Neurology (HTC, SKS, CJ); Department of Pathology (WJK); and PET Center (BA, HTC, OM, DCC, SKS, CEB, CJ), Children's Hospital of Michigan, Wayne State University School of Medicine, Detroit, MI.

ABSTRACT

BACKGROUND AND PURPOSE

We used L-[1–^{11}C]leucine (LEU) positron emission tomography (PET) to measure amino acid uptake in children with Sturge-Weber syndrome (SWS), and to relate amino acid uptake measures with glucose metabolism.

METHODS

LEU and 2-deoxy-2[^{18}F]fluoro-D-glucose (FDG) PET were performed in 7 children (age: 5 months-13 years) with unilateral SWS. Asymmetries of LEU uptake in the posterior brain region, underlying the angioma and in frontal cortex, were measured and correlated with glucose hypometabolism. Kinetic analysis of LEU uptake was performed in 4 patients.

RESULTS

Increased LEU standard uptake value (SUV, mean: 15.1%) was found in the angioma region in 6 patients, and smaller increases in LEU SUV (11.5%) were seen in frontal cortex in 4 of the 6 patients, despite normal glucose metabolism in frontal regions. High LEU SUV was due to both increased tracer transport (3/4 patients) and high protein synthesis rates (2/4). FDG SUV asymmetries in the angioma region were inversely related to LEU SUV asymmetries ($r = -.83$, $P = .042$).

CONCLUSIONS

Increased amino acid uptake in the angioma region and also in less affected frontal regions may provide a marker of pathological mechanisms contributing to chronic brain damage in children with SWS.

Keywords: Sturge-Weber syndrome, positron emission tomography, leucine, proliferation, glucose metabolism.

Acceptance: Received March 12, 2010, and in revised form July 27, 2010. Accepted for publication September 19, 2010.

This study was supported by a grant from the National Institutes of Health (R01 NS041922 to CJ).

The authors report no conflict of interest.

Correspondence: Address correspondence to Csaba Juhász, MD, PhD, Departments of Pediatrics and Neurology, Wayne State University, PET Center, Children's Hospital of Michigan, 3901 Beaubien Blvd, Detroit, MI 48201. E-mail: juhasz@pet.wayne.edu.

J Neuroimaging 2012;22:177-183.
DOI: 10.1111/j.1552-6569.2010.00565.x

Introduction

Sturge-Weber syndrome (SWS) is a sporadic neurocutaneous disorder characterized by a facial port wine stain and leptomeningeal angiomatosis. The abnormal, tortuous veins on the cortical surface lead to impaired cerebral blood flow, hypoxia, and chronic ischemia of the underlying brain tissue.[1,2] The often progressive neurological complications include hemiparesis, visual field defects, seizures, and mental retardation.[3] Leptomeningeal angiomas are generally considered to be developmental malformations, the results of a failed regression of the primitive embryonal vascular plexus during the first trimester of gestation.[4] Recent studies, however, suggested that these angiomas may not be static lesions but, may undergo dynamic proliferative changes.[5,6] These studies have provided evidence for increased expression of vascular cell proliferation markers in the resected angioma and brain tissue. Histological studies have shown neuronal degeneration, gliosis, and calcification in the brain tissue adjacent to the angioma in SWS.[5,7] These degenerative changes are consistent with decreases in glucose metabolism demonstrated by positron emission tomography (PET).[8]

Increased cell proliferation has been studied in vivo using PET to measure glucose metabolic rates, amino acid uptake (to measure protein synthesis), and uptake of thymidine analogs (to measure DNA synthesis); these approaches are commonly used in the clinical setting to estimate proliferative activity of malignancies.[9,10] In brain tumors, amino acid uptake generally provides a more accurate estimate of proliferative activity than measures of glucose metabolism.[11,12]

Among several available amino acid PET tracers, ^{11}C-labeled leucine is very suitable to estimate tissue protein synthesis rates because of its kinetic modeling.[13,14] In this study, we measured L-[1–^{11}C]leucine (LEU) uptake in angioma regions and in brain regions not directly affected by the angioma in children with SWS who had unilateral, predominantly posterior, brain involvement associated with seizures. We hypothesized that the posterior brain regions, affected directly by the angioma, would show increased uptake of LEU on PET. To evaluate potential pathological correlates of abnormal amino acid uptake in the angioma region, histopathological features, including vascular proliferative activity and glial markers, were assessed directly in a resected angioma of an infant who underwent hemispherectomy following LEU PET. In addition, we hypothesized that higher increases of LEU uptake would be associated with more severe glucose metabolic abnormalities, measured by 2-deoxy-2[^{18}F]fluoro-D-glucose (FDG) PET, due to more severe tissue damage underlying the angioma.

Materials and Methods

Subjects

Seven children (5 boys, age range: 5 months-13 years, median age: 6 years at the time of LEU PET; Table 1) with the clinical and radiological diagnosis of SWS who had unilateral hemispheric involvement and history of seizures underwent MR imaging as well as PET scanning using the tracers FDG and LEU in the Children's Hospital of Michigan, Detroit. These children were selected from a series of 48 consecutive children with SWS who were recruited between October 2004 and August 2009 for a prospective neuroimaging research study, including yearly clinical and imaging follow-ups, approved by the Institutional Review Board at Wayne State University. All selected patients (15% of the recruited patients) met the following inclusion criteria: (1) age below 14; (2) radiologic (magnetic resonance imaging [MRI] and FDG PET) evidence of unilateral brain involvement; (3) history of seizures; (4) no evidence of seizure(s) during PET; (5) parents' approval for a second PET scan (LEU) in addition to FDG PET and MRI. Five patients had right hemispheric, whereas two patients had left hemispheric involvement. In one patient (patient no. 5), leptomeningeal angioma could not be visualized on MRI; however, the presence of a right facial port wine stain as well as right central transmedullary veins indicated right hemispheric involvement. Some imaging studies were collected 1 year apart from each other (see Table 1) as the patients participated in a prospective, longitudinal study with yearly follow-ups (except the infant who underwent hemispherectomy after initial imaging). The MRI and FDG PET image data, which were the closest to the LEU PET scan in time, were used for analysis (Table 1). FDG and LEU PET scans were done at the same time (1 day apart) in 5 patients and 1 year apart in the remaining two (patients no. 4 and no. 7). These latter patients were 5 and 11.8 years old at the time of the first scan; thus, both of them were older than 3 years when major metabolic progression had been observed.[15] Written informed consent was obtained from the parents or legal guardians.

FDG PET Data Acquisition

All PET scans were performed using a CTI/Siemens EXACT/HR scanner (Siemens, Knoxville, TN). This scanner has a 15 cm field of view and generates 47 image planes with a slice thickness of 3.125 mm. The FDG PET scanning protocol has been described in detail previously.[16] The reconstructed in-plane resolution is 5.5 mm (±.35) full width at half maximum and 6.0 mm (±.49) in the axial direction. Initially, a venous line was established to inject FDG (.143 mCi/kg). After 40 minutes of FDG uptake, a static 20-minute emission scan of the brain was acquired in 3-dimensional (3D) mode. Calculated attenuation correction was applied to the brain images using automated threshold fits to the sinogram data. All FDG PET scans were performed in the interictal state as indicated by EEG monitoring performed during the FDG uptake period.

LEU PET Data Acquisition

The tracer L-[^{11}C]-leucine was produced at Children's Hospital of Michigan using a synthesis module designed and built in

Table 1. Clinical and Imaging Data of the Patients

Patient No.	Age (years)	Sex	PWS side	Initial Imaging	Imaging 1 Year Later	Angioma Location	FDG AI (Posterior; %)	FDG AI (Frontal; %)	LEU SUV AI (Kcompl AI/VD AI) (Posterior; %)	LEU SUV AI (Kcompl AI/VD AI) (Frontal; %)
1	.4	F	Right	MRI, FDG, Leu	n.a.[†]	rFTPO	–28.5	.5	35.2* (n.a.)	16.3* (n.a.)
2	2.4	F	Left	MRI (FDG)	FDG, Leu	lTPO	–45.2	–1.3	12.1* (8.7*/32.8*)	6.9* (–1.5/47.2*)
3	2.9	M	Right	MRI (FDG)	FDG, Leu	rTPO	–2.9	1.7	8.2* (6.5*/37.1*)	1.4 (–2.5/26.4)
4	6.0	F	Left	FDG (MRI)	MRI, Leu	lTPO	–61.2	–9.2	12.0* (n.a.)	8.8* (n.a.)
5	7.3	M	Right	MRI (FDG)	FDG, Leu	[right trans-med. veins]	3.2	1.7	–1.5 (–3.7/19.3)	–1.6 (.2/–8.7)
6	10.7	M	Right	MRI	FDG, Leu	rTPO	–90	2.5	13.9* (1.6/57.8*)	.4 (–1.2/–8.2)
7	12.8	M	Right	MRI, FDG	Leu	rFTPO	–53.7	–6.9	8.9* (n.a.)	14.1* (n.a.)

[†]Patient had hemispherectomy after initial imaging studies.

Note: Age is given at the time of L-[1–^{11}C]leucine PET.

F = female; M = male; PWS = port wine stain; r = right; l = left; F = frontal; T = temporal; P = parietal; O = occipital; FDG = 2-deoxy-2[^{18}F]fluoro-D-glucose, LEU = L-[1–^{11}C]leucine; transmed. = transmedullary; SUV = standardized uptake value; Kcompl = K-complex macroparameter; VD = volume of distribution; AI = asymmetry index; n.a. = not available. Imaging studies in parenthesis were not used for this study. Values exceeding the corresponding normal mean AI ± 3SD are indicated with an asterisk.

house.[17] Details of the imaging procedure have been described previously.[14] Four of the 7 patients had blood input data obtained during the PET study for more detailed quantification. The PET sequence began with a transmission scan of the chest. Subsequently, the tracer L-[1–^{11}C]-leucine (.1 mCi/kg) was injected, and a 20-minute dynamic PET scan of the heart was performed (sequence: 12 × 10 s, 3 × 60 s, 3 × 300 s) in order to obtain the left ventricular (LV) input function. Continuation of the input function was then accomplished by combining the time-activity curve derived from a small region-of-interest (ROI) in the center of the LV with venous blood samples obtained at later times. Subsequently, beginning at 25 minutes following tracer injection, seven 5-minute scans of the brain were performed in 3D mode followed by a 15-minute transmission scan of the brain. Measured attenuation, scatter, and decay correction were applied to all PET images. Scalp EEG was not monitored during the LEU uptake period.

MRI Data Acquisition

All MRI studies were carried out on a Sonata 1.5 T MRI scanner (Siemens, Erlangen, Germany) using a standard head coil. For the purpose of the present study, only the postgadolinium T1-weighted images (T1-Gad) were used (as a reference for coregistration of PET images). The acquisition parameters of this sequence were as follows: TR/TE:20/5.6 ms; flip angle: 25°; voxel size: 1 × .5 × 2 mm^3.

Sedation during Imaging Studies

Children aged <2 years were sedated with chloral hydrate (50-100 mg/kg by mouth), and children aged 2-8 years were sedated with nembutal (3 mg/kg), followed by fentanyl (1 μg/kg), as necessary. All sedated subjects were continuously monitored by pediatric nurses, and physiological parameters (heart rate, pulse oximetry, respiration) were measured during the studies.

ROI Definition

FDG PET images as well as summed and individual frames of the LEU PET images were initially rigid-body coregistered to each patient's T1-Gad MR images using a 3D registration technique (VINCI 2.50).[18] Subsequently, ROIs encompassing the angioma region (including the angioma and the underlying cortex; these structures were not delimited separately, since they cannot be distinguished on PET images due to their close proximity) as well as mirror regions in the contralateral hemisphere were defined on the gadolinium-enhanced MRI images using ROI Editor 1.4.1 (www.mristudio.org). All these regions were located mainly in the posterior (temporal, parietal, occipital) cortex. In patient no. 5, with no leptomeningeal angioma visualized on MRI, similar posterior cortex was included in this ROI. In addition, ROIs were drawn on at least three image planes in apparently spared (no atrophy and angioma) or less affected (mild hypometabolism in some cases; see Table 1) frontal cortical regions ipsilateral to the angioma as well as in contralateral homotopic regions. All ROIs were then superimposed on the coregistered FDG and LEU PET images including the dynamic LEU image sequences, in cases where blood input data were available. In subjects, who had MRI and PET scans acquired 1 year apart, small manual adjustments of the ROIs had to be carried out to adjust for interim changes in brain size.

Semi-Quantitative Analysis of FDG and LEU Uptake

Standardized uptake values (SUVs) for FDG and LEU uptake were calculated for all regions by dividing the average radioactivity concentration obtained from each region by the injected FDG and LEU dose per total body weight, respectively. Subsequently, asymmetry indices (AIs) for SUVs were calculated as follows: AI (%) = 200 × [(I − C)/(I + C)], where I represents ipsilateral, C represents contralateral values as compared to the side of the lesion. For FDG, AI values above 10% were considered to be abnormal.[15,16] For LEU, normal control asymmetries were calculated using LEU PET images of five healthy adults (all males, mean age: 39 years), where absolute values of right-left SUV AIs were calculated for both posterior and frontal regions, separately, and AI values above the normal mean ± 3 standard deviations (SDs) were considered to be abnormal in the patients. We used the conservative 3 SDs because of the unknown age-related differences in normal AIs of cortical LEU uptake.

Quantitative Analysis of Protein Synthesis

To study mechanisms of LEU uptake abnormalities, unidirectional uptake rate constant (K-complex) and volume of distribution (VD) were derived from the Patlak graphical analysis[19] in 4 cases where blood input data were available. Details of this approach have been described previously.[14] Asymmetries (AIs) for K-complex and VD were calculated similar to those for SUVs. Again, AI values above the normal mean ± 3 SDs, derived from the normal controls, were considered to be abnormal. Absolute SUV, K-complex, and VD values of the patients were not compared to those of the healthy adults due to potential developmental differences in cerebral protein synthesis rates.[20]

Statistical Analysis

Hemispheric asymmetries in the angioma and frontal regions were compared using Wilcoxon's signed-rank test. Association between glucose metabolic and LEU uptake asymmetries was tested using Spearman's rank correlation. $P < .05$ was considered statistically significant.

Histological assessment of resected tissue samples

Resected specimens were available from one patient, an infant who underwent hemispherectomy at 6 months of age. In addition to standard histological processing of the resected brain and angioma tissues (including hematoxylin-eosin, cresyl violet, Masson trichrome, glial fibrillary acidic protein [GFAP], and synaptophysin immunostaining, Luxol fast-blue/periodic-acid Schiff), angioma specimens were also immunostained using Ki-67 antibody (clone K-2, Ventana), colabeled with the endothelial marker CD31 (JC70A, Ventana, Tucson, AZ, USA) to demonstrate proliferative activity in the endothelial cells of the angioma.[6,21] Furthermore, the expression of vascular endothelial growth factor-A (VEGF-A) was also assessed (using mouse antihuman monoclonal antibodies; sc-7269, Santa Cruz Inc., Santa Cruz, CA, USA) in the resected angioma specimen.

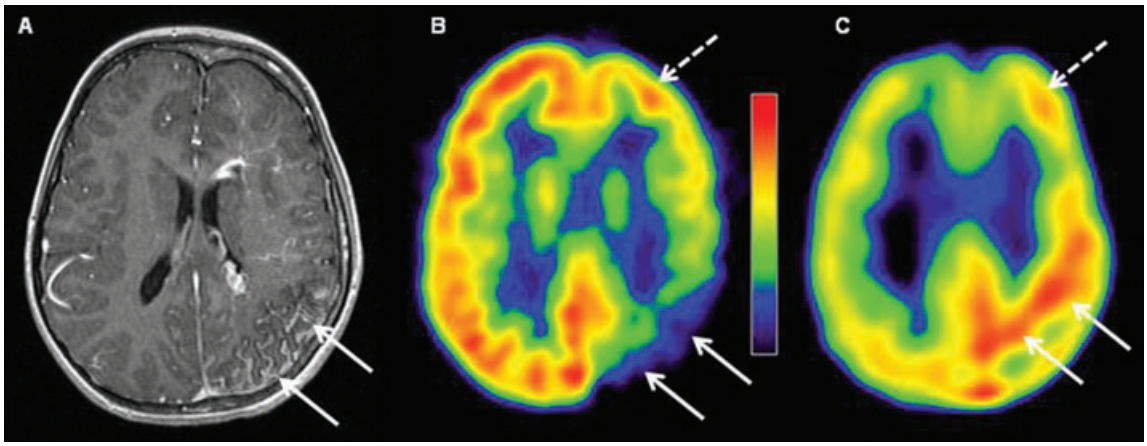

Fig 1. Representative co-registered T1 postgadolinium MRI (A), FDG PET (B), and L-[1–^{11}C]leucine (LEU) PET (C) images of a 6-year-old girl (patient no. 4) with left hemispheric angioma in the temporo-parieto-occipital region. Solid arrows indicate the angioma region, which was hypometabolic (AI = –61%) but showed abnormally increased LEU uptake (AI = 12%). Although the MRI showed deep transmedullary veins in the frontal lobe, the angioma did not extend to the frontal cortex. However, this region was also mildly hypometabolic (dashed arrow; AI = 9%) and showed moderately increased LEU uptake (SUV AI = 9%) compared to the contralateral homotopic area.

Immuno-histochemistry results of resected brain tissues of 7 (non-SWS) patients (age range: 4 months-7 years), who underwent epilepsy surgery, are also presented for comparison.

Results

FDG and LEU Uptake Asymmetries

LEU SUV asymmetries in the angioma and frontal regions exceeded the calculated normal cutoff values (3.8% for the angioma region and 3.3% for frontal cortex) in 6 and 4 cases, respectively (mean AIs for these abnormal cases: angioma–15.1%, frontal–11.5%; see Fig 1). FDG SUV asymmetries were abnormal (>10%) in 5 patients in the angioma region (mean AI: 55.7%) and in none of the patients in the frontal region. Glucose metabolic asymmetries of the angioma region were significantly higher than those of the frontal regions (–39.7% vs. –2.3%; $P = .028$). However, LEU uptake asymmetries of the angioma region were only slightly higher than those of the frontal regions (12.7 vs. 6.6%; $P = .09$).

Quantification of LEU Uptake

Four patients had blood input data to estimate regional protein synthesis rates. K-complex asymmetries exceeded the normal AI limit (angioma region: 4.8%; frontal: 4.4%) in the 2 youngest children (ages: 2.4 and 2.9 years) where quantification was available in the angioma region (increases; AI: 8.7% and 6.5%, respectively) and in none of the cases in the frontal cortex (Table 1). VD asymmetry was above the normal AI limit (angioma region: 28%, frontal: 30%) in the angioma region in 3 patients and in the frontal region in 1 child, always with higher values ipsilateral to the angioma.

Association between Glucose Hypometabolism and LEU Uptake

We found a significant negative correlation between FDG SUV asymmetries and LEU SUV asymmetries for the 6 patients older than 2 years of age in the angioma regions ($r = –.83$, $P = .042$, see Fig 2) and a trend for the same association in the frontal regions ($r = –.77$; $P = .07$), indicating that higher LEU uptake was associated with more severe hypometabolism. For this analysis, we excluded patient no. 1, a 5-month-old infant. In this age group, patients with SWS often show increased glucose metabolism and blood flow, followed by a transition from

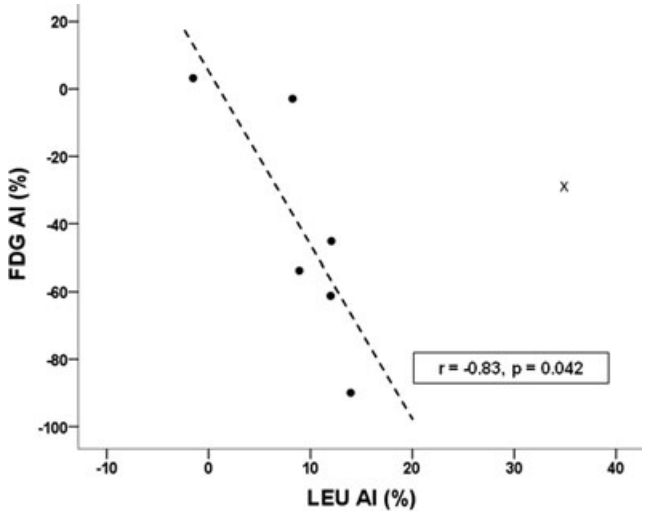

Fig 2. Relationship between glucose metabolic (FDG) versus L-[1–^{11}C]leucine (LEU) uptake asymmetries (AIs) in the angioma region. Black circles represent datapoints from the six older (above the age of 2 years) patients with chronic disease. A correlation for these patients' data indicates that higher LEU uptake ipsilateral to the angioma is associated with more severe glucose hypometabolism ($r = –.83$, $P = .042$). In addition, the cross indicates the data of an infant with recent onset seizures. This case was not included in the correlation since glucose uptake is not an appropriate measure of cortical damage in the initial stage of the disease when potential transition of cortical hypermetabolism to hypometabolism occurs.

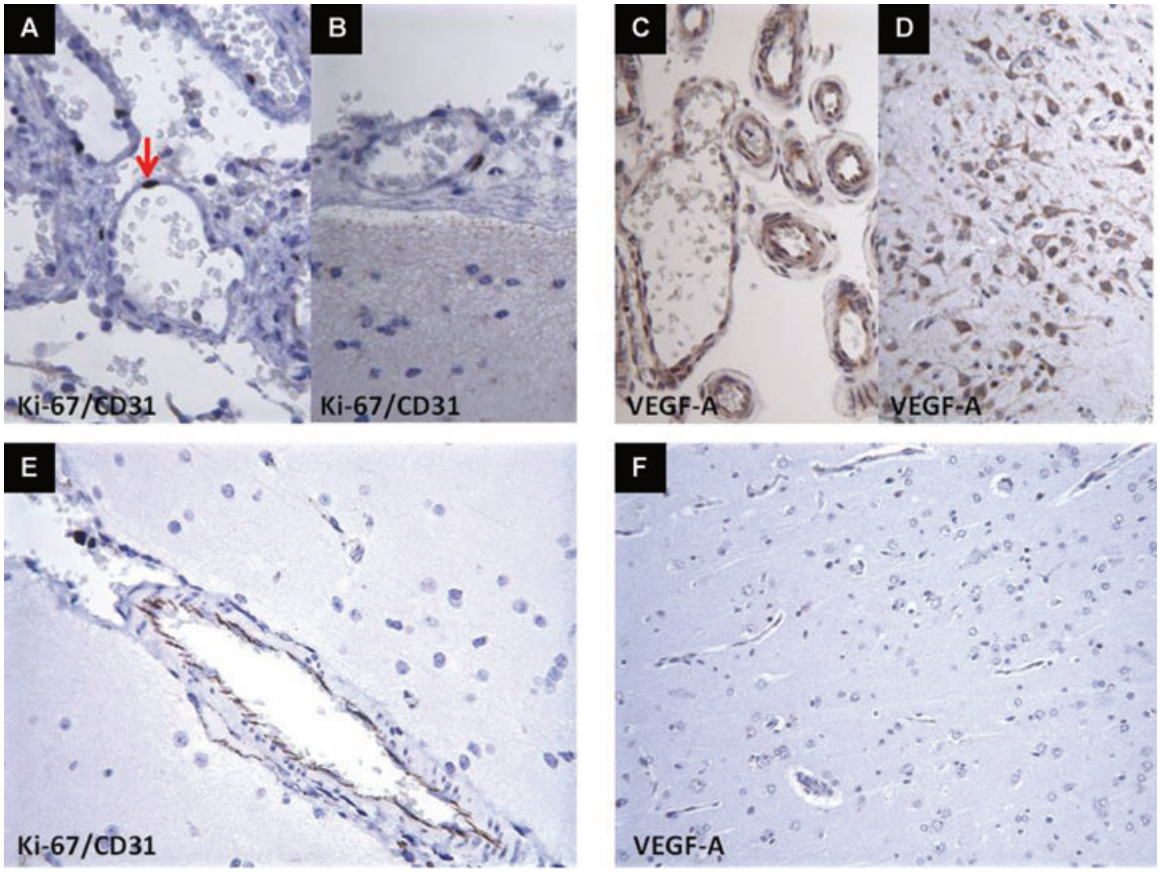

Fig 3. Immunostaining for the proliferation marker Ki-67 (costained with endothelial marker CD31; A) and VEGF-A (C) in resected angioma tissue as well as cortex (B and D) of an infant (patient no. 1) who underwent hemispherectomy at 6 months of age. These representative images show positive Ki-67 labeling (brown stain) in numerous endothelial nuclei of the leptomeningeal angioma (one of the Ki-67 positive nuclei is shown by a red arrow) as well as intense VEGF-A staining (brown) in leptomeningeal vessels. No Ki-67 staining was seen in the cortex but numerous cells showed VEGF-A expression. The representative images at the bottom show no endothelial Ki-67 expression (E) and no neuronal staining for VEGF (F) in tissue samples of one of the control subjects (a 4-year-old patient with intractable temporal lobe epilepsy).

increased to decreased metabolism and blood flow.[22] This patient's data point may be an outlier (see point denoted by X in Fig 2) in this comparison for this reason.

Histopathological Assessment

The surgical specimen from the infant who underwent epilepsy surgery showed marked leptomeningeal vascularity, cortical malformation (polymicrogyria and heterotopias), neuronal loss, gliosis (positive GFAP immunostaining), and prominent calcification. Positive Ki-67 labeling was seen in the nuclei of endothelial cells (Fig 3A) but not in cortical cells (Fig 3B). The calculated proliferative index (proportion of labeled endothelial cells) was between 5% and10%. In comparison, no endothelial Ki-67 staining was seen in control tissues (Fig 3E). In addition, we also found strong VEGF-A expression in endothelial cells of the angioma as well as in cortical neurons (Figs 3C, D). Pediatric epilepsy control tissues showed no, or weak, staining for VEGF (Fig 3F).

Discussion

The main finding of this study is the increased LEU SUV of the angioma region and in the frontal lobe in some cases in children with SWS. Based on the available data with quantification, these increases are driven by elevated VD of labeled leucine indicating elevated LEU transport in 3 of the 4 cases and also by increased protein synthesis rates reflected by the K-complex in 2 of the 4 cases. These results increase our understanding of pathological changes occurring in brain underlying the angioma and beyond in frontal cortical regions showing relatively normal glucose metabolism. Elevations in amino acid transport and protein synthesis may be related to endothelial and glial proliferation, which were observed in the one case in which brain tissue was available for pathological studies. Altered blood-brain barrier (BBB) is also a probable mechanism for increased amino acid uptake near the angioma. Further studies are needed to understand these mechanisms more fully.

This is a preliminary study with a limited number of subjects. Additional major limitations include that FDG and LEU PET images were acquired 1 year apart from each other in some cases. Furthermore, detailed kinetic analysis could be carried out in only a subset of the study group. Importantly, the angioma and the underlying cortex could not be distinguished on the PET images since partial volume effects preclude the reliable separate analysis of these structures. Therefore, our results most likely represent a summed effect of abnormal amino acid

transport and protein synthesis in these structures, at least in the angioma-affected regions. In addition, changes in glucose metabolism during development in the region of the angioma complicate our analysis. In SWS, FDG PET often detects profound cortical hypometabolism of the affected hemisphere, predominantly under the angioma but frequently extending well beyond the apparent structural abnormalities seen on MRI.[16,22] We found a significant inverse association between the severity of hypometabolism and the increase in LEU uptake in children above 2 years of age. In the only infant (a 5-month-old boy), LEU uptake showed the highest AI value, while FDG AI was relatively moderate. However, this latter may not reflect the true degree of tissue damage in this young age, as infants with SWS are known to show transient hypermetabolism,[22] followed by a transition from hyper- to hypometabolism in the affected brain regions. Therefore, it is possible that in this infant, FDG PET underestimated the severity of cortical involvement. In the 6 older children, higher LEU uptake associated with lower glucose metabolism suggests that the degree of amino acid transport and protein synthesis (related to BBB damage, glial, or vascular proliferation) is associated with tissue damage as reflected by low glucose metabolism.

Recent studies have demonstrated that intracranial vascular malformations in SWS are not static lesions but may undergo dynamic remodeling.[5] Enhanced endothelial cell turnover as well as increased expression of key angiogenetic factors, such as VEGF and its receptor, provided evidence for ongoing angiogenesis and suggested the progressive nature of angiomas.[5,6] In addition to the leptomeningeal angioma, the structure and neural regulation of cortical vessels are also affected in this disorder.[23,24] Whether these vascular changes contribute to clinical disease progression remains to be clarified.

In our study, the increased LEU uptake in the angioma region was mainly driven by the increase in the VD of the tracer, suggesting increased amino acid transport. The marked increase of LEU VD may be due to the retention of the amino acid by increased vascular beds, disruption of the BBB, increased capillary permeability, and/or increased expression of the large amino acid transporter (LAT1).[23,25] Contrast enhancement of the leptomeningeal angioma on MRI suggests BBB disruption, which itself can lead to increased amino-acid uptake.[26] Increased uptake of two other amino-acid tracers (ie, ^{11}C-methionine and α-[^{11}C]methyl-L-tryptophan, where increased VD, but not high K-complex, was associated with contrast enhancement) has been demonstrated in brain tumors and other pathological conditions associated with BBB breakdown.[27,28] In contrast, FDG uptake is not sensitive to BBB disruption,[29,30] thus, glucose metabolic rates on PET may remain low even in the case of impaired BBB. Accumulation of ^{11}C-methionine (which, similar to leucine, is a substrate of LAT1) on PET was reported in the angioma region of an adult with SWS,[25] but quantification of methionine uptake has not been performed. The mechanism of the increase in the K-complex macroparameter also remains to be determined. Based on a study from Comati et al. and our previous work demonstrating proliferative activity and angiogenesis in the vascular malformations,[5,6] increased protein synthesis may be expected in the angioma due to active remodeling. This is supported by immuno-histochemistry findings in our youngest patient, showing endothelial Ki-67 proliferative index of 5-10%, similar to what could be expected in low-grade tumors.[31] Importantly, other factors, such as cortical glial proliferation or increased expression and deposition of extracellular matrix proteins such as fibronectin[4] could also contribute to high protein synthesis in the angioma region. In addition, cortical malformations (also seen in our infant) have been reported in patients with SWS[32] and these epilepsy-associated developmental abnormalities can show increased amino acid uptake.[33] Detection of such malformations by imaging could be of high clinical importance in SWS as these lesions are highly epileptogenic and should be considered when partial resection is planned in children with SWS and intractable epilepsy. Although mechanisms of increased LEU uptake are currently speculative and warrant further studies, our imaging findings suggest that increased LEU uptake on PET may be a useful marker of underlying pathology not only in angioma-affected regions but also in frontal cortex even when it shows no apparent abnormalities on conventional imaging in children with SWS.

This study was supported by a grant from the National Institutes of Health (R01 NS041922 to CJ). The content is solely the responsibility of the authors and does not necessarily represent the official views of the NIH. The authors thank Thomas Mangner, PhD and Pulak Chakraborty, PhD for the reliable radiosynthesis of the PET tracers. We are also grateful to Galina Rabkin, CNMT, Angie Wigeluk, CNMT, and Carole Klapko, CNMT for their expert technical assistance in performing the PET studies and to Anna Deboard RN for performing sedation. We also thank the Sturge-Weber Foundation for referring patients to us. We are grateful to the families and children who participated in the study.

References

1. Bentson JR, Wilson GH, Newton TH. Cerebral venous drainage pattern of the Sturge-Weber syndrome. *Radiology* 1971;101:111-118.
2. Lin DD, Barker PB, Hatfield LA, et al. Dynamic MR perfusion and proton MR spectroscopic imaging in Sturge-Weber syndrome: correlation with neurological symptoms. *J Magn Reson Imaging* 2006;24:274-281.
3. Roach E, Bodensteiner J. Neurologic manifestations of Sturge-Weber syndrome. In: Bodensteiner JB, Roach ES, eds. *Sturge-Weber Syndrome*. Mt. Freedom, NJ: The Sturge-Weber Foundation,1999:27-38.
4. Comi AM. Pathophysiology of Sturge-Weber syndrome. *J Child Neurol* 2003;18:509-516.
5. Comati A, Beck H, Halliday W, et al. Upregulation of hypoxia-inducible factor (HIF)-1α and HIF-2α in leptomeningeal vascular malformations of Sturge-Weber syndrome. *J Neuropathol Exp Neurol* 2007;66:86-97.
6. Batista C, Kupsky W, Chugani D, et al. Endothelial cell proliferation and angiogenesis in Sturge-Weber syndrome. *Ann Neurol* 2008;64(Suppl 12):119-120 [abstract].
7. Norman MG, Schoene WC. The ultrastructure of Sturge-Weber disease. *Acta Neuropathol* 1977;37:199-205.
8. Juhász C, Haacke EM, Hu J, et al. Multimodality imaging of cortical and white matter abnormalities in Sturge-Weber syndrome. *AJNR Am J Neuroradiol* 2007;28:900-906.
9. Barwick T, Bencherif B, Mountz JM, et al. Molecular PET and PET/CT imaging of tumour cell proliferation using F-18

fluoro-L-thymidine: a comprehensive evaluation. *Nucl Med Commun* 2009;30:908-917.
10. Plathow C, Weber WA. Tumor cell metabolism imaging. *J Nucl Med* 2008;49(Suppl 2):43S-63S.
11. Giammarile F, Cinotti LE, Jouvet A, et al. High and low grade oligodendrogliomas (ODG): correlation of amino-acid and glucose uptakes using PET and histological classifications. *J Neurooncol* 2004;68:263-274.
12. Kato T, Shinoda J, Nakayama N, et al. Metabolic assessment of gliomas using ^{11}C-methionine, [^{18}F] fluorodeoxyglucose, and ^{11}C-choline positron-emission tomography. *AJNR Am J Neuroradiol* 2008;29:1176-1182.
13. Bishu S, Schmidt KC, Burlin T, et al. Regional rates of cerebral protein synthesis measured with L-[1–^{11}C]leucine and PET in conscious, young adult men: normal values, variability, and reproducibility. *J Cereb Blood Flow Metab* 2008;28:1502-1513.
14. Sundaram SK, Muzik O, Chugani DC, et al. Quantification of protein synthesis in the human brain using L-[1–^{11}C]-leucine PET: incorporation of factors for large neutral amino acids in plasma and for amino acids recycled from tissue. *J Nucl Med* 2006;47:1787-1795.
15. Juhász C, Batista CE, Chugani DC, et al. Evolution of cortical metabolic abnormalities and their clinical correlates in Sturge-Weber syndrome. *Eur J Paediatr Neurol* 2007;11:277-284.
16. Lee JS, Asano E, Muzik O, et al. Sturge-Weber syndrome: correlation between clinical course and FDG PET findings. *Neurology* 2001;57:189-195.
17. Mu F, Mangner T, Chugani H. Facile synthesis of L-[1–^{11}C]leucine as a PET radiotracer for the measurement of cerebral protein synthesis. *J Labelled Compds Radiopharm* 2005;48:S189.
18. Cizek J, Herholz K, Vollmar S, et al. Fast and robust registration of PET and MR images of human brain. *Neuroimage* 2004;22:434-442.
19. Patlak CS, Blasberg RG, Fenstermacher JD. Graphical evaluation of blood-to-brain transfer constants from multiple-time uptake data. *J Cereb Blood Flow Metab* 1983;3:1-7.
20. Hovda DA, Villablanca JR, Chugani HT, et al. Metabolic maturation of the brain: a study of local cerebral protein synthesis in the developing cat. *Brain Res* 2006;1113:54-63.
21. Batista CE, Juhász C, Muzik O, et al. Imaging correlates of differential expression of indoleamine 2,3-dioxygenase in human brain tumors. *Mol Imaging Biol* 2009;11:460-466.
22. Chugani HT, Mazziotta JC, Phelps ME. Sturge-Weber syndrome: a study of cerebral glucose utilization with positron emission tomography. *J Pediatr* 1989;114:244-253.
23. Di Trapani G, Di Rocco C, Abbamondi AL, et al. Light microscopy and ultrastructural studies of Sturge-Weber disease. *Childs Brain* 1982;9:23-36.
24. Cunha e Sa M, Barroso CP, Caldas MC, et al. Innervation pattern of malformative cortical vessels in Sturge-Weber disease: an histochemical, immunohistochemical, and ultrastructural study. *Neurosurgery* 1997;41:872-876; discussion 876-877.
25. Ichinose T, Tsuyuguchi N, Morino M, et al. Discrepancy between [^{18}F]fluorodeoxyglucose and ^{11}C-methionine positron emission tomography findings in Sturge-Weber syndrome–case report. *Neurol Med Chir (Tokyo)* 2003;43:461-464.
26. Singhal T, Narayanan TK, Jain V, et al. ^{11}C-L-methionine positron emission tomography in the clinical management of cerebral gliomas. *Mol Imaging Biol* 2008;10:1-18.
27. Dethy S, Manto M, Kentos A, et al. PET findings in a brain abscess associated with a silent atrial septal defect. *Clin Neurol Neurosurg* 1995;97:349-353.
28. Juhász C, Chugani DC, Muzik O, et al. In vivo uptake and metabolism of α-[^{11}C]methyl-L-tryptophan in human brain tumors. *J Cereb Blood Flow Metab* 2006;26:345-357.
29. Roelcke U, Radu EW, von Ammon K, et al. Alteration of blood-brain barrier in human brain tumors: comparison of [^{18}F]fluorodeoxyglucose, [^{11}C]methionine and rubidium-82 using PET. *J Neurol Sci* 1995;132:20-27.
30. Spaeth N, Wyss MT, Pahnke J, et al. Uptake of ^{18}F-fluorocholine, ^{18}F-fluoro-ethyl-L: -tyrosine and ^{18}F-fluoro-2-deoxyglucose in F98 gliomas in the rat. *Eur J Nucl Med Mol Imaging* 2006;33:673-682.
31. Torp SH, Alsaker M. Ki-67 immunoreactivity, basic fibroblastic growth factor (bFGF) expression, and microvessel density as supplementary prognostic tools in low-grade astrocytomas. An immunohistochemical study with special reference to the reliability of different Ki-67 antibodies. *Pathol Res Pract* 2002;198:261-265.
32. Maton B, Krsek P, Jayakar P, et al. Medically intractable epilepsy in Sturge-Weber syndrome is associated with cortical malformation: implications for surgical therapy. *Epilepsia* 2010;51:257-267.
33. Sasaki M, Kuwabara Y, Yoshida T, et al. Carbon-11-methionine PET in focal cortical dysplasia: a comparison with fluorine-18-FDG PET and technetium-99m-ECD SPECT. *J Nucl Med* 1998;39:974-977.